Polymer - Carbon Nanotube Composites for Thermoelectric Applications

J. Luo, B. Krause[a)] and P. Pötschke[b)]

Leibniz-Institut für Polymerforschung Dresden e.V., Hohe Straße 6, 01069 Dresden, Germany

[a)] krause-beate@ipfdd.de
[b)] Corresponding author: poe@ipfdd.de

Abstract. The thermoelectric (TE) performance of electrically conductive thermoplastic composites prepared by melt mixing was investigated. A cost effective widely used in industry polymer, namely polypropylene (PP), was chosen as the matrix to fabricate the composites. Singlewalled carbon nanotubes (SWCNTs), the amount (2 wt%) of which was selected to be above the electrical percolation threshold (< 0.2 wt%), were used to form an electrical conducting network. Besides as produced SWCNTs plasma modified tubes were employed to study the influence of the functionalization on the morphology, dispersion and TE properties of the PP composites. In addition, melt processing conditions, e.g. temperature, rotation speed, and mixing time were varied. Furthermore, an ionic liquid (IL, 1-methyl-3-octylimidazolium tetrafluoroborate) was used as a processing additive during melt mixing, which was confirmed to improve the electrical conductivity of the composites. Simultaneous increase in the Seebeck coefficient was recorded, leading to a much better power factor compared to composites without IL. This melt mixing strategy opens new avenues for solvent-free, large scale fabrication of polymer based TE materials.

INTRODUCTION

Nanometer sized fillers are widely embedded into polymer matrices to fabricate functional nanocomposites. These nanofillers include carbon nanomaterials (e.g. carbon nanotubes and carbon black), metal nanoparticles, oxides, etc. In particular, composites with carbon nanomaterials are well developed as electrically conductive polymer composites (CPC) for diverse applications. For instance, carbon nanomaterials based composites are mainly employed for the dissipation of static electricity, floor heating elements, and electronic parts such as electromagnetic interference (EMI) shielding [1]. Besides these traditional applications, CPCs are developed as thermoelectric materials to turn waste heat into electrical energy.

The thermoelectric (TE) effect (also called Seebeck effect) is described as an electrical potential (voltage ΔU) induced by a temperature difference (ΔT) between the two sides of a material. Accordingly, the Seebeck coefficient (S) of the material is defined as

$$S = -\Delta U / \Delta T \tag{1}$$

The Seebeck coefficient is an intrinsic material property and independent of the sample geometry. The free charge carriers inside the material determine the sign of the Seebeck coefficient. A negative Seebeck coefficient (N-type) implies dominant electron carriers while positive Seebeck coefficient (P-type) shows dominant hole carriers. The TE performance of a material is evaluated by a dimensionless figure of merit, ZT, which is given as [2]

$$ZT = \sigma^2 ST / \kappa \tag{2}$$

with σ as the electrical conductivity, κ as the thermal conductivity and $\sigma^2 S$ represents the power factor (PF). An efficient TE material should have high electrical conductivity and a Seebeck coefficient (resulting in a high PF). At the same time, low thermal conductivity is required.

Traditional TE materials are based on semiconductors, e.g. Bi_2Te_3. These materials are heavy and contain toxic rare earth elements (Te). Despite their high PF, these materials have high thermal conductivity, for instance, 1.2 to 1.6 W/(m·K) for a commercial Bi_2Te_3 crystal [3]. Sophisticated and high energy demanding techniques are required to reduce the value below 1 W/(m·K) [4]. Polymer materials, on the other hand, have intrinsic low thermal conductivity in the range of 0.1 to 0.6 W/(m·K) [5]. Furthermore, the light weight and flexibility of polymers make them very attractive in the integration of TE materials into portable devices for power supply [6]. Nevertheless, the challenge in polymer based TE materials is to achieve high PF. With their high electrical conductivity, intrinsic conjugated polymers have been intensively investigated. In particular, poly(3,4-ethylenedioxythiophene) (PEDOT) is reported to have a metallic electrical conductivity over 3000 S/cm by a post treatment with sulfuric acid [7,8].

However, the Seebeck coefficient of this polymer is usually in the range of 20 µV/K [9,10]. By reducing the oxidation level of PEDOT, the Seebeck coefficient of PEDOT film could be increased up to 200 µV/K and a high PF of 324 $\mu W/(m\cdot K^2)$ was obtained [11]. However, the reduction in the oxidation level resulted in a concurrent drop in the electrical conductivity [11-14]. As a result, it is only possible to obtain an optimized PF by the oxidation level control. This intercoupling behavior between the Seebeck coefficient and electrical conductivity is similar to what occurs by doping in semiconductor based TE materials.

Polymer composites filled with nanoparticles provide another promising approach to improve the TE performance by the choice of different fillers. In this case, both insulating and electrical conducting polymers are applicable. These fillers could be either organic such as carbon nanotubes (CNTs) [15-18] and graphene [19] for higher electrical conductivity, or inorganic semiconductors such as Bi_2Te_3 nanoparticles [20,21], Te nanowires [22] and PbTe nanoparticles [23] for a higher Seebeck coefficient. These composites are typically fabricated by solution mixing in an organic solvent. Compared to solution mixing, melt mixing technique can be easily scaled up to industry level and it avoids the usage of organic solvents. Nevertheless, due to the low electrical conductivity of composites with insulating polymer matrix, the TE properties of melt mixed composites are rarely studied. Antar et al. reported the TE performance of multiwalled CNTs and expanded graphite filled melt mixed poly(lactic acid) composites, in which the highest Seebeck coefficient is 17 µV/K at 32 vol% expanded graphite and the highest PF is $9.6x10^{-2}$ $\mu W/(m\cdot K^2)$ at 18 vol% CNTs [24]. Our previous work focused on the influence of the surface functionalization of multiwalled CNTs on TE properties of melt mixed polymer nanocomposites based on polycarbonate (PC), in which the highest Seebeck coefficient was below 12 µV/K and the electrical conductivity was below 0.1 S/cm even at 2.5 wt% CNT [25]. Furthermore, a cyclic butylene terephthalate (CBT) oligomer was utilized to successfully improve both the processing and electrical conductivity of PC/CNT nanocomposites [26]. Nevertheless, the Seebeck coefficients of all investigated samples are still below 14 µV/K.

As all reported Seebeck coefficients of melt mixed composites are extremely low, the focus of our work was to improve the Seebeck coefficient by a selection of different types of SWCNTs. At the same time, the CNT concentration and the processing conditions were investigated. An ionic liquid (IL, 1-methyl-3-octylimidazolium tetrafluoroborate) was previously reported to improve both the dispersion and electrical conductivity of CNTs for melt mixed polymer composites, e.g. in PMMA [27], rubber [28] and polyamide [29]. Therefore, it was employed during the processing of the composites to study its influence on the TE properties.

EXPERIMENTS AND CHARACTERIZATIONS

Polypropylene (PP) Moplen HP400R (LyondellBasell Industries), different types (A, B and mA) of SWCNTs (> 75% purity, Tuball^{TM}, OCSiAl Ltd) with diameters of 1-2 nm and length larger than 5 µm [30] and ionic liquid (IL) 1-methyl-3-octylimidazolium tetrafluoroborate (purity >97%, HPLC, Sigma Aldrich) were used. SWCNT type A and B represent as synthesized SWCNTs prepared at different synthesis parameters. SWCNTs of type A were plasma oxidized to produce the mA type SWCNTs.

A conical twin-screw microcompounder (DSM Xplore 15) with a capacity of 15 ccm was used for melt mixing. The weight percentage of CNTs was calculated regarding the whole composite. CNTs were manually mixed with IL in an agate mortar with the ratio of CNT/IL fixed to 1:1. Afterwards, mixtures of grounded PP powders (diameter <1 mm) and defined amounts of CNTs and IL pre-shaken in glass vial, were fed into the running microcompounder. The standard processing conditions were fixed to a melting temperature of 210°C, a rotation speed of 250 rpm and a mixing time of 5 min. The melting temperature and rotation speed were modified as it is specified in the sample notation to study the influence of processing condition. Afterwards, these mixed composites were pressed at 210°C under a pressure of 50 kN into circular plates with a diameter of 60 mm and a thickness of 0.3 mm using a press PW 40 EH (Paul Otto Weber GmbH, Germany). Rectangular samples were manually cut from the pressed circular plates and used for the electrical conductivity and Seebeck coefficient.

For conductivity characterization, a 4-electrode test fixture combined with a Keithley electrometer E6517A or Keithley multimeter DMM2000 was used. The reported electrical conductivities are the averaged value of eight measurements for each sample. The Seebeck coefficient at room temperature was determined using a measurement platform SRX [31] and the results are the average of at least 3 measurements for each sample. For samples with CNT content < 0.8 wt%, the equipment is not able to give reliable values due to the high electrical resistance, thus, no results are presented. SEM investigations of cryo-fractured surfaces (deposited with a thin layer of carbon) were performed using a Gemini 1530 microscope.

RESULTS AND DISCUSSION

Figure 1 shows the TE properties of melt processed composites containing plasma oxidized CNTs (type mA) [32]. With an increasing amount of CNTs inside the insulating PP matrix an electrical conducting network is built up starting already at 0.2 wt%. Further addition of CNTs results in only a slight increase in electrical conductivity, which saturates above a content of 4 wt% CNTs. As CNTs are the only conductive parts in these composites, the Seebeck coefficients are determined by the SWCNTs. All composites (> 0.8 wt% CNT) display positive Seebeck coefficients due to the p-type characteristic of CNTs [33]. The increase in electrical conductivity with CNT concentration is attributed to the injected charge carriers by the CNTs. However, the increased charge carrier concentration is detrimental for the Seebeck coefficient, leading to a slight reduction tendency with the CNT content. The highest power factor of 6.6×10^{-2} $\mu W/(m \cdot K^2)$ is observed for composites containing 4 wt% CNTs due to the intercoupling behavior between the Seebeck coefficient and electrical conductivity.

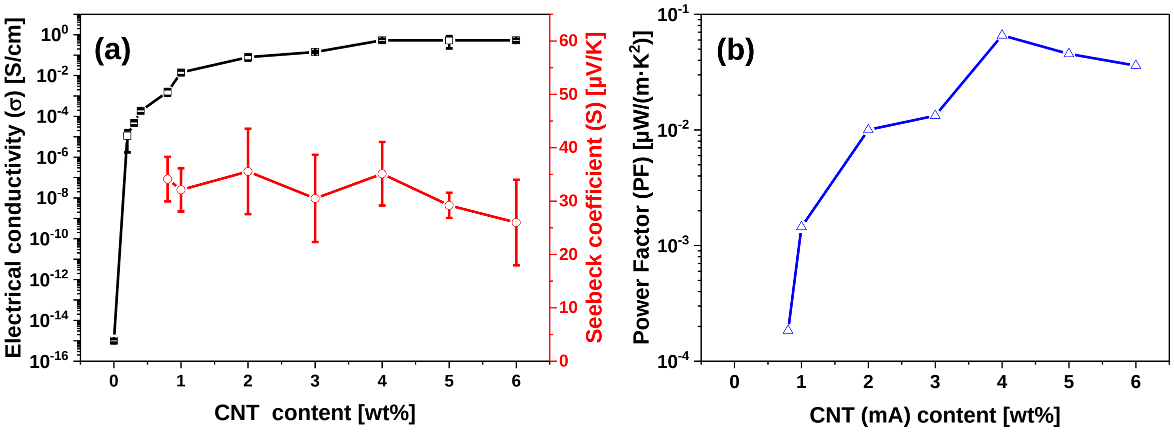

FIGURE 1. Thermoelectric properties of PP composites versus SWCNT concentration (type mA) [32].

In addition, two types of nonfunctionalized SWCNTs (types A and B) were investigated. At the same time, IL was added as dispersing agent during the melt mixing. The CNT concentration in the composites was kept at 2 wt%. As it is shown in Figure 2, the use of nonfunctionalized CNTs results in higher electrical conductivity than that of plasma functionalized CNTs (type mA). However, the plasma oxidation increases the Seebeck coefficient of the composite from 23.2 µV/K (for CNTs type A) to 35.6 µV/K (for CNTs type mA). Nevertheless, this change results in only small increase in the PF. Compared to A and mA types of SWCNTs, the addition of SWCNTs (type B) generates composites with much higher electrical conductivity and Seebeck coefficient, leading to a much higher PF (Table 1).

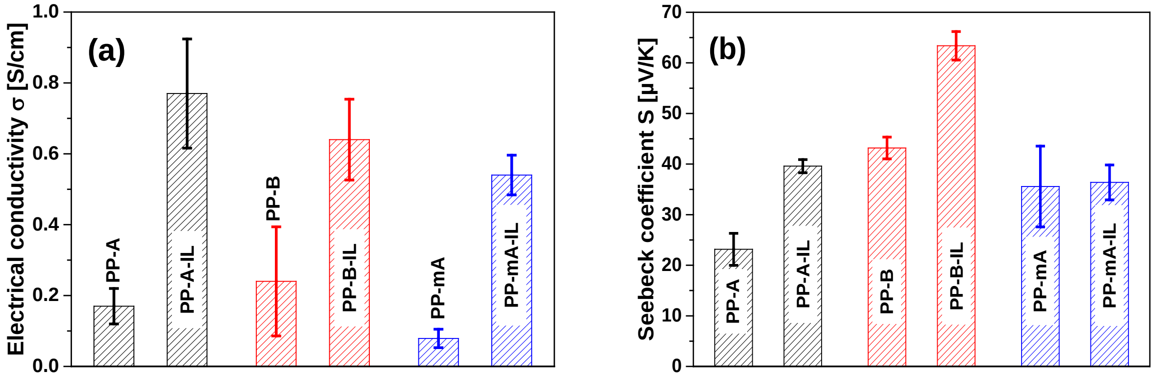

FIGURE 2. The influence of CNT type and IL addition on the TE properties of CPCs with 2 wt% CNTs (SWCNT:IL=1:1).

Simultaneous increase in the electrical conductivity and Seebeck coefficient is evidenced for all three types of SWCNTs when IL was added during mixing. The enlargement in the PF is determined by the SWCNT type. The addition of IL only slightly increases the PF of the composite filled with B type CNTs, which already has a high value without IL. On the other hand, for composites containing CNTs prepared with the same synthesis condition (types A and mA), the enhancement in the PF by IL addition is much higher. Nevertheless, the composite with B type CNTs and IL shows the highest Seebeck coefficient (63 µV/K) and PF (0.26 µW/(m·K^2)).

TABLE 1. Influence of CNT type and IL addition on the power factor of PP composites with 2 wt% SWCNTs and 2 wt% IL.

Material	Power Factor PF [µW/(m·K^2)]
PP-A	0.009
PP-A-IL	0.12
PP-B	0.12
PP-B-IL	0.26
PP-mA	0.01
PP-mA-IL	0.07

As the addition of SWCNTs (B type) results in composites with the highest PF, morphological investigations of corresponding composites filled with or without IL are shown in Figure 3. Long SWCNTs are well dispersed inside the PP matrix. Holes in the SEM images are assigned to IL as it is liquid at room temperature and immiscible with the PP matrix. Nevertheless, it is difficult to distinguish the difference of the CNT dispersion state between composites with and without IL and to prove the expected better dispersion as seen in previous studies [27-29].

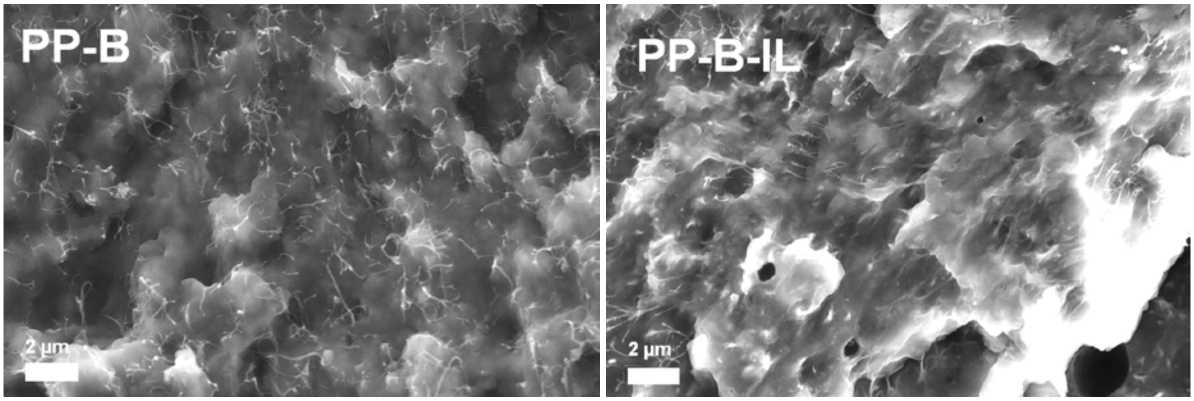

FIGURE 3. SEM of cryofractured surfaces of the composites PP-B and PP-B-IL (2 wt% SWCNTs and 2 wt% IL).

The influence of processing condition was investigated using samples containing mA Type SWCNTs. Reduction of mixing speed from 250 rpm to 100 rpm, which results in lower shear stresses during mixing, slightly reduced the electrical conductivity, but increased the Seebeck coefficient. Increasing the melt mixing temperature from 210 to 230°C showed only an effect at 100 rpm, where lower electrical conductivity, Seebeck coefficient and PF were measured for samples mixed at the higher mixing temperature. The maximum Seebeck coefficient and PF were obtained by the combination of low mixing temperature (210°C) and low rotation speed (100 rpm) where, interestingly, the electrical conductivity was not the highest among all variations. However, in summary, the processing conditions do not affect much of the TE properties of these composites.

TABLE 2. Influence of processing condition on the composites filled with 2 wt% SWCNTs type mA and 2 wt% IL.

Material	Electrical conductivity [S/cm]	Seebeck coefficient [µV/K]	Power Factor PF [µW/(m·K^2)]
PP-mA-IL-250rpm-210°C-5	0.54	36.4	0.072
PP-mA-IL-100rpm-210°C-5	0.47	45.6	0.098
PP-mA-IL-250rpm-230°C-5	0.54	36.7	0.073
PP-mA-IL-100rpm-230°C-5	0.41	42.2	0.073

CONCLUSIONS

Electrically conductive melt mixed polymer composites containing SWCNTs are suitable materials for the use in TE applications. Compatible P-and N-type materials based on melt mixed PP composite system were applied to produce a prototype of thermoelectric generator (TEG) to demonstrate the applicability of melt mixing to fabricate TE materials [34].

Even if the achieved values for the Seebeck coefficient and power factor are still far below those for traditional TE materials, the strategy of incorporating conductive carbon nanostructures is promising for future applications, especially when low price, light weight and high flexibility of polymer based composites are taken into consideration. The influence of structural properties of CNTs and their dispersion are factors which must be studied more in detail. The use of the dispersing additive IL was shown to improve not only state of dispersion, but also electrical conductivity, the Seebeck coefficient and the corresponding power factor.

ACKNOWLEDGMENTS

We thank OCSiAl Ltd for providing the different kinds of SWCNTs Tuball^{TM}.

REFERENCES

1. T. Tanka, G. C. Montanari and R. Mülhaupt, IEEE Trans. Dielectr. Electr. Insul., **11**, 763-784 (2004).
2. D. M. Rowe, “General Principles and Basic Considerations,” in *Thermoelectrics Handbook: Macro to Nano*, edited by D. M. Rowe (CRC Press, Boca Raton,2005), pp. 1-14.
3. http://www.everredtronics.com/thermoelectric.P.N.pellets.html
4. B. Poudel, Q. Hao, Y. Ma, Y. Lan, A. Minnich, B. Yu, X. Yan, D. Wang, A. Muto, D. Vashaee, X. Chen, J. Liu, M. S. Dresselhaus, G. Chen and Z. Ren, Science **320**, 634-638 (2008).
5. J. E. Mark, *Physical Properties of Polymers Handbook* (Springer-Verlag, New York, 2007)
6. B. T. McGrail, A. Sehirlioglu and E. Pentzer, Angew. Chem. Int. Ed. **54**, 1710-1723 (2015).
7. N. Kim, H. Kang, J. H. Lee, S. Kee, S. H. Lee and K. Lee, Adv. Mater. **27**, 2317-2323 (2015).
8. Y. Xia, K. Sun and J. Ouyang, Adv. Mater. **24**, 2436-2440 (2012).
9. J. H. Bahk, H. Fang, K. Yazawa and A. Shakouri, J. Mater. Chem. C **3**, 10362-10374 (2015).
10. Q. Zhang, Y. Sun, W. Xu and D. Zhu, Adv. Mater. **26**, 6829-6851 (2014).
11. B. Bubnova, Z. U. Khan, A. Malti, S. Braun, M. Fahlman, M. Berggren and X. Crispin, Nat. Mater. **10**, 429-433 (2011).
12. O. Bubnova, M. Berggren and X. Crispin, Journal of the American Chemical Society **134**, 16456-16459 (2012).
13. H. Park, S. H. Lee, F. S. Kim, H. H. Choi, I. W. Cheong and J. H. Kim, J. Mater. Chem. A **2**, 6532-6539 (2014).
14. S. H. Lee, H. Park, W. Son, H. H. Choi and J. H. Kim, J. Mater. Chem. A **2**, 13380-13387 (2014).
15. Y. Choi, Y. Kim, S. G. Park, Y. G. Kim, B. J. Sung, S. Y. Jang and W. Kim, Org. Electron. **12**, 2120 (2011).
16. C. A. Hewitt, A. B. Kaiser, S. Roth, M. Craps, R. Czerw and D. L. Carroll, Nano Lett. **12**, 1307-1310 (2012).
17. Q. Yao, L. Chen, W. Zhang, S. Liufu and X. Chen, ACS Nano **4**, 2445-2451 (2010).
18. C. Yu, K. Choi, L. Yin and J. C. Grunlan, ACS Nano **5**, 7885-7892 (2012).
19. G. H. Kim, D. H. Hwang and S. I. Woo, Phys. Chem. Chem. Phys. **14**, 3530-3536 (2012).
20. M. He, J. Ge, Z. Lin, X. Feng, X. Wang, H. Lu, Y. Yang and F. Qiu, Energy Environ. Sci. **5**, 8351-8358 (2012).
21. Y. Du, K. F. Cai, S. Chen, P. Cizek and T. Lin, ACS Appl. Mater. Interfaces **6**, 5735-5743 (2014).
22. N. E. Coates, S. K. Yee, B. McCulloch, K. C. See, A. Majumdar, R. A. Segalman and J. J. Urban, Adv. Mater. **25**, 1629-1633 (2013).
23. Y. Wang, K. Cai and X. Yao, ACS Appl. Mater. Interfaces **3**, 1163-1166 (2011).
24. Z. Antar, J. F. Feller, H. Noël, P. Glouannec and K. Elleuch, Mater. Lett. **67**, 210-214 (2012).
25. M. Liebscher, T. Gärtner, L. Tzounis, M. Micusik, P. Pötschke, M. Stamm, G. Heinrich and B. Voit, Compos. Sci. Technol. **101**, 133-138 (2014).
26. L. Tzounis, T. Gärtner, M. Liebscher, P. Pötschke, M. Stamm, B. Voit and G. Heinrich, Polymer **55**, 5381 (2014).
27. L. Zhao, Y. Li, X. Cao, J. You and W. Dong, Nanotechnol. **23**, 255702 (2012).
28. K. Subramaniam, A. Das, K. W. Stöckelhuber and G. Heinrich, Rubber Chem. Technol. **86**, 367-400 (2013).
29. R. Socher, *PA12-MWCNT-Nanokomposite: Wege zur effektiven MWCNT-Dispergierung und zu niedrigen elektrischen Perkolationsschwellen*. (Verlag Dr. Huth, München, 2013).
30. B. Krause, P. Pötschke, E. Ilin and M. Predtechenskiy, Polymer **98**, 45-50 (2016).
31. http://www.ipm.fraunhofer.de/en/services/contract-measurements/thermoelectric-measurements.html
32. J. Luo, B. Krause and P. Pötschke, AIMS Mater. Sci. 3, 1107-1116 (2016).
33. M. Shim, A. Javey, N. W. S. Kam and H. Dai, J. Am. Chem. Soc. **123**, 11512-11513 (2001).
34. J. Luo, G. Cerretti, B. Krause, L. Zhang, T. Otto, W. Jenschke, M. Ullrich, W. Tremel, B. Voit and P. Pötschke, Polymer **108**, 513-520 (2017).